

Reactivity of Bulky Formamidinosamarium(II or III) Complexes with C=O and C=S Bonds[#]

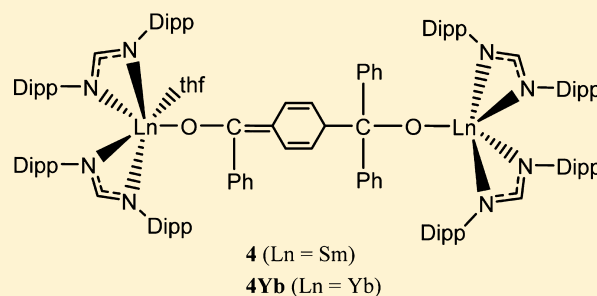
Glen B. Deacon,^{*,†} Peter C. Junk,^{*,‡} Jun Wang,^{†,‡} and Daniel Werner[†]

[†]School of Chemistry, Monash University, Victoria, 3800, Australia

[‡]College of Science, Technology & Engineering, James Cook University, Townsville, Queensland 4811, Australia

S Supporting Information

ABSTRACT: The preparation of a new heterobimetallic samarium(II) formamidinate complex and selected reactions of samarium(II) complexes and one samarium(III) formamidinate complex with benzophenone or CS₂ are discussed. Treatment of the tris(formamidinato)samarium(III) complex [Sm(DippForm)₃] **1** (DippForm = *N,N'*-bis(2,6-diisopropylphenyl)formamidinate, (CH₃(NC₆H₃-*i*Pr₂-2,6)₂) with potassium graphite in toluene yielded the dark brown heterobimetallic formamidinosamarium(II)/potassium complex [KSm(DippForm)₃]_n **2**. Divalent **2**, a Lewis base solvent free homoleptic species, differs significantly from the related heteroleptic formamidinosamarium(II) complex [Sm(DippForm)₂(thf)₂] **3** with respect to its constitution, structure, and reactivity toward benzophenone. While **2** reacts giving complex **1**, the reaction of **3** with benzophenone generates the highly unusual [Sm(DippForm)₂(thf){μ-OC(Ph)=C(C₆H₅)-C(Ph)₂O}Sm(DippForm)₂] (C₆H₅ = 1,4-cyclohexadiene-3-yl-6-ylidene) **4**. The formation of **4** highlights a rare C–C coupling between a carbonyl carbon and the carbon at the para position of a phenyl group of the OCPH₂ fragment. An analogous reaction of [Yb(DippForm)₂(thf)₂] gives an isostructural complex **4Yb**. **3** reacts with carbon disulfide forming a light green dinuclear formamidinosamarium(III) complex [{Sm(DippForm)₂(thf)}₂(μ-η²(C,S):κ(S',S'')-SCSCS₂)] **5** through an unusual C–S coupling induced by an amidinatolanthanoid species giving the thioformylcarbonotrithioate ligand. The trivalent organometallic [Sm(DippForm)₂(CCPh)(thf)] complex activates the C=O bond of benzophenone by an insertion reaction, forming the light yellow [Sm(DippForm)₂{OC(Ph)₂C₂Ph}(thf)] **6** as a major product and light yellow unsolvated [Sm(DippForm)₂{OC(Ph)₂C₂Ph}] **7** as a minor product. Molecular structures of complexes (**2**, **4**–**7**) show that κ(*N,N'*) bonding between a DippForm and samarium atom exists in all compounds, but in **2**, DippForm also bridges K and Sm by 1κ(*N*):2κ(*N'*) bonding and two 2,6-diisopropylphenyl groups are η⁶-bonded to potassium.



INTRODUCTION

The reactivity of divalent samarium complexes has captured the interest of researchers from various chemistry disciplines.¹ Commercially available samarium(II) diiodide, widely used as a single electron reducing agent in organic reaction processes,² underpins the applications of reactive samarium(II) compounds. Upon coordination by organic moieties, samarium(II) species can have enhanced reduction potential (cf. Sm³⁺/Sm²⁺, *E*_{1/2} = −1.55 V, and Sm^{III}Cp₃/Sm^{II}Cp₃[−], −2.50 V).³ Divalent organosamarium complexes have been found to possess high reactivity toward unsaturated chemical bonds including some of the most unreactive such as the N≡N bond.⁴

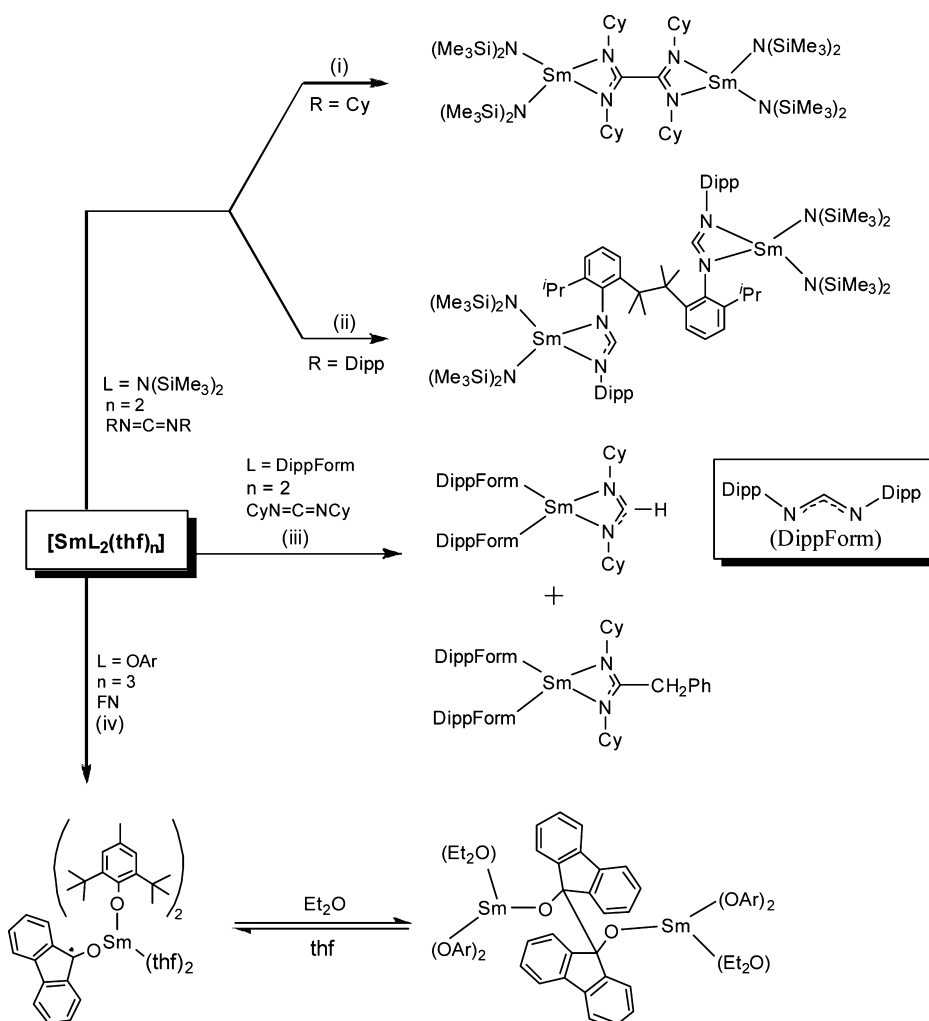
Previously we have reported reduction reactions of the divalent samarium complex [Sm(N(SiMe₃)₂)₂(thf)₂] with C=N bonds in carbodiimides to form either a dinuclear oxalamidinate ((RN)₂CC(NR)₂) (Scheme 1i) through C–C coupling of the central diimide carbon atoms of RNCNR fragments,⁵ a dinuclear diformamidinate complex (Scheme 1ii) formed through coupling of two methine carbon atoms of ^{*i*}Pr groups,⁵ or mononuclear formamidinate complexes (Scheme 1iii), formed by C–H activation of solvent toluene by

[Sm(DippForm)₂(thf)₂] (DippForm = *N,N'*-bis(2,6-diisopropylphenyl)formamidinate, CH₃(NC₆H₃-*i*Pr₂-2,6)₂).⁶ These processes demonstrated that the size of the carbodiimide substrate and the ligation of samarium(II) fundamentally alter the outcome of related reduction reactions. We have also investigated the contrasting reaction type of phenylethynylsamarium(III) complexes with carbodiimides, where C≡N bonds were activated in insertion reactions.⁶

Targeting a C=O bond in a molecule such as fluorenone, divalent samarium complexes induce reduction and usually form pinacolate complexes through C–C coupling (Scheme 1iv).⁷ The process involves ketyl intermediates which are isolable when well stabilized.^{7–9} In contrast, the parallel reactions with benzophenone were attempted but mainly led to an unisolable product mixture.¹⁰ However, the successful transformation by reductive C–C coupling to form isolable pinacolate complexes was induced by [Yb(NCS)₂(thf)₂]¹¹ and a magnesium(II) 1,2-bis{(2,6-diisopropylphenyl)imino}-

Received: September 7, 2014

Scheme 1. Reactions between Divalent Samarium Complexes and Carbodiimides (RNCNR, R = Cyclohexyl (Cy)), 2,6-Diisopropylphenyl (Dipp), or 9-Fluorenone (FN)^a

^aOAr = 2,6-di-*tert*-butyl-4-methylphenolate.

acenaphthenate.¹² When CO₂ was treated with [SmCp*₂(thf)₂] (Cp* = pentamethylcyclopentadienyl), reductive coupling gave an oxalate complex,¹³ but a different pathway was identified when utilizing a macrocyclic *N,N'*-dimethyl-*meso*-octaethylcalix[4]pyrrolate–samarium(II) complex. In the latter, C=O bonds cleave, giving a carbonate complex and CO as coproduct.^{13b,14} Targeting a C=S bond, [SmCp*₂(thf)₂] reacts with COS, yielding a disproportionation product [Cp*₂Sm(μ-κ(S,S')):2κ(O)-S₂CO)SmCp*₂(thf)] and CO.¹³ The transformation of CS₂ by organolanthanoids has only recently been explored in the reaction with [Sm^(III)(Giso)₂] (Giso = [(ArN)₂CNCy₂], Ar = 2,6-diisopropylphenyl, Cy = cyclohexyl), which was observed to form [(Giso)₂Sm(μ-η²(C,S):κ(S',S'')-SCSCS₂)Sm(Giso)₂].^{15a} The product was shown to be formed through C–S coupling, but some uncertainty remained about the bonding modes of the central (SCSCS₂) moiety due to the limited quality of crystallography data. An entirely different outcome results from the reaction of [K₂Ln(OSi(O-^{*i*}Bu)₃)₄] (Ln = Yb, Eu) with CS₂, which process yields K₂CS₃ (+CS), K₂C₂S₄ and K₂C₃S₅ as the sulfur containing products.^{15b} The transformations of CS₂ by d-metal complexes mainly result in C–C coupling (yielding

tetrathiooxalate $[\text{S}_2\text{CCS}_2]^{2-}$),¹⁶ but C-S couplings have also occasionally been observed.¹⁷

Extending our studies of *N*-donor alternatives to the cyclopentadienyl family of ligands,¹⁸ we now report the synthesis of a rare Lewis base free heterobimetallic formamidinatosamarium(II) complex [KSm(DippForm)₃]_n **2**, and the reactivity of divalent samarium complexes **2** and [Sm(DippForm)₂(thf)₂] **3** with benzophenone as well as the analogous reaction of [Yb(DippForm)₂(thf)₂]. The reaction of **3** with CS₂ is also described. In addition we report the activation of the C=O bond in benzophenone by a phenylethynylsamarium(III) complex, thereby providing a contrast to reductive activation of **2** and **3**.

■ EXPERIMENTAL SECTION

The compounds described herein were prepared and handled using conventional inert atmosphere techniques with dinitrogen gas. IR spectra were recorded as Nujol mulls between NaCl plates using either a PerkinElmer 1600 series FTIR instrument or a PerkinElmer Spectrum RX I FTIR spectrometer within the range 4000–600 cm^{-1} . ^1H NMR spectra were recorded on a Bruker DPX 300 spectrometer, and chemical shifts were referenced to the residual ^1H resonances of the deuterated solvents. Melting points were determined in sealed glass capillaries under nitrogen and are uncalibrated.

Microanalyses were determined by the Campbell Microanalytical Service, University of Otago (New Zealand), or Elemental Analysis Service of London Metropolitan University (U.K.). Solvents used for reactions were predried over sodium metal and distilled over sodium for toluene or sodium benzophenone ketyl for thf and hexane. NMR solvent C_6D_6 was degassed and dried over sodium with stirring overnight and filtered before use. Benzophenone and carbon disulfide were purchased from Merck, potassium was purchased from Chem Supply, and they were used as supplied. $[Sm(DippForm)_3]_1$,⁶ potassium graphite,¹⁹ $H(DippForm)$,²⁰ SmI_2 (0.1 M solution in thf),²¹ $[Yb(DippForm)_2(thf)_2]$,²² $[Sm(DippForm)_2Cl(thf)]$,²³ and $[Sm(DippForm)_2(CPh)(thf)]$ ²⁴ were prepared by literature methods.

Synthesis of $[KSm(DippForm)_3]_2$. Toluene (20 mL) was added to a Schlenk flask charged with tris(formamidinato)samarium complex $[Sm(DippForm)_3]_1$ (0.62 g, 0.50 mmol) and potassium graphite (0.10 g, 0.75 mmol). The mixture was stirred at 90 °C for 0.5 h and kept at this temperature for 0.5 h. The mixture was filtered at this temperature, and the volume of the brown colored solution was reduced to 5 mL under vacuum. On storage at ambient temperature for 2 days, dark brown crystalline 2-1.25PhMe precipitated and was collected after decanting the solution (yield: 0.42 g, 61%), mp 302–306 °C. IR (Nujol)/ cm^{-1} : 1593 m, 1530 s, 1358 m, 1311 s, 1253 m, 1228 w, 1180 m, 1157 w, 1109 w, 1055 w, 1039 w, 991 w, 922 m, 882 w, 820 w, 801 w, 779 w, 772 w, 754 m, 694 w, 674 w. Anal. Calcd (%) for $C_{83.75}H_{115}N_6KSm$ (1395.27): C, 72.09; H, 8.31; N, 6.02. Found: C, 71.55; H, 8.19; N, 6.04.

Reaction of $[KSm(DippForm)_3]_2$ with benzophenone. Toluene (1 mL) was added to a Schlenk flask charged with $[KSm(DippForm)_3]_2$ (0.14 g, 0.1 mmol) and benzophenone (18 mg, 0.1 mmol). The mixture was warmed to dissolve both reagents, and the mixture was stored for 2 weeks at ambient temperature, during which time light yellow needle crystals precipitated and were collected (yield: 30 mg, 22%). The unit cell measurement for the crystals showed that they were $[Sm(DippForm)_3]^{25}$ space group $P2_1/n$, $a = 13.136(2)$, $b = 37.816(7)$, $c = 16.395(3)$ Å, $\beta = 96.386(30)^\circ$, $V = 8093.70$ Å³.

Synthesis of $[Sm(DippForm)_2(thf)_2]_3$. The compound was synthesized by a modified literature procedure:²⁵ thf (50 mL) was added to a Schlenk flask charged with potassium metal (0.16 g, 4.1 mmol) and $H(DippForm)$ (1.46 g, 4.0 mmol). The mixture was heated to reflux for 3 h with stirring and then cooled to ambient temperature. SmI_2 (0.10 M solution in thf, 20 mL, 2.0 mmol) was added dropwise with stirring, and the mixture was stirred overnight. Thf was removed in vacuo and replaced by toluene (50 mL). The resulting slurry was stirred for half an hour. After standing overnight, the mixture was filtered. The dark green filtrate was concentrated in vacuo to ca. 20 mL and stored at –10 °C for 1 week, during which time dark green crystals precipitated and were collected (yield: 1.60 g, 78%). ¹H NMR (300 MHz, C_6D_6 , 303 K): –12.78 (br s, 2H, NCHN), 1.17 (br s, 8H, $CH(CH_3)_2$), 3.09 (br s, 48H, $CH(CH_3)_2$), 3.78 (s, 8H, $CH_2(thf)$), 4.47 (d, $J = 7.2$ Hz, 8H, Ar-m-H), 6.17 (t, $J = 7.1$ Hz, 4H, Ar-p-H), 11.42 (br s, 8H, $OCH_2(thf)$). The ¹H NMR spectrum was similar to that reported.⁶

Transformation of $[Sm(DippForm)_2Cl(thf)]$ into 3. C_6D_6 (0.7 mL) was added to a J. Young valve equipped NMR tube charged with $[Sm(DippForm)_2Cl(thf)]$ (0.030 g) and potassium graphite (0.030 g). The mixture was shaken by hand at ambient temperature for 1 min. ¹H NMR spectroscopy identified that 3 was formed.

Transformation of $[KSm(DippForm)_3]_2$ into 3. C_6D_6 (0.7 mL) was added to a J. Young valve equipped NMR tube charged with $[KSm(DippForm)_3]_2$ (0.030 g) and one drop of thf. The mixture was shaken by hand and warmed to complete the transformation of 2. ¹H NMR spectroscopy identified that 3 was formed.

Synthesis of $[(DippForm)_2(thf)Sm\{\mu-OC(Ph)C_6H_5\}C(Ph)_2O]_4Yb$. A solution of benzophenone (0.10 g, 0.50 mmol) in toluene (5 mL) was added with stirring to a Schlenk flask charged with a green solution of $[Sm(DippForm)_2(thf)_2]_3$ (0.50 g, 0.50 mmol), in toluene (10 mL) at ambient temperature. The color of the solution turned purple, and the mixture was stirred continuously for half an hour. The volume of solution was reduced to 2 mL under

vacuum, hexane (5 mL) was added, and the mixture was stored at ambient temperature for 2 days, during which time a pale solid precipitated and was collected by decanting of the solution. The solid was dried under vacuum and crystallized from 1 mL of toluene, giving crystalline colorless 4-2.5PhMe (yield: 0.33 g, 54%), mp 142 °C (dec). IR (Nujol)/ cm^{-1} : 1666 m, 1593 w, 1515 m, 1316 w, 1276 s, 1188 m, 1159 w, 1140 m, 1112 w, 1056 w, 1042 w, 932 w, 898 w, 867 w, 798 m, 766 m, 752 m, 700 m, 642 w, 625 w. Anal. Calcd (%) for $C_{147.5}H_{188}N_8O_3Sm_2$ (2421.76): C, 73.15; H, 7.82; N, 4.63. Found: C, 72.99; H, 6.91; N, 4.35.

Synthesis of $[(DippForm)_2(thf)Yb\{\mu-OC(Ph)C_6H_5\}C(Ph)_2O]_4Yb$. $[Yb(DippForm)_2(thf)_2]$ (0.75 g, 0.71 mmol) and benzophenone (0.13 g, 0.71 mmol) were dissolved in thf (3 mL) in a Schlenk flask. After 5 min, hexane was added (2 mL) to the deep purple solution and the flask was heated to 40 °C. Upon concentration in vacuo (1 mL) and cooling to room temperature, small dichroic yellow/red crystals of 4Yb-2.25thf were isolated suitable for single crystal X-ray crystallography analysis. The sample was further dried under vacuum, leaving a light yellow powder (yield: 0.57 g, 67%), mp 220–226 °C. IR (Nujol): 1665 m, 1638 w, 1595 m, 1579 m, 1560 m, 1519 vs, 1501 s, 1401 w, 1318 s, 1276 vs, 1235 w, 1193 w, 1160 w, 1142 m, 1093 vs, 1066 vs, 1046 s, 1020 s, 946 vw, 933 vw, 899 vw, 801 s, 766 s, 755 s, 723 vw, 701 m. Anal. Calcd (%) for $C_{139}H_{186}N_8O_{5.25}Yb_2$ (2399.04): C, 69.59; H, 7.81; N, 4.67. Found: C, 69.61; H, 7.62; N, 4.85.

Synthesis of $[Sm(DippForm)_2(thf)_2]\{\mu-\eta^2(C,S): \kappa(S',S'')-SCSCS_2\}_5$. Carbon disulfide (one drop) was added at ambient temperature to a Schlenk tube charged with a dark green solution of $[Sm(DippForm)_2(thf)_2]_3$ (51 mg, 0.05 mmol), in deuterated benzene (0.8 mL). The solution was shaken gently for 1 min, and the color of the solution gradually turned bright green. The solution was then stored at ambient temperature for 2 days, during which time light green crystalline 5-6 C_6D_6 was collected (yield: 30 mg, 47%), mp 160 °C (dec). IR (Nujol)/ cm^{-1} : 1588 w, 1520 s, 1460 s, 1316 m, 1286 m, 1253 w, 1234 w, 1186 m, 1099 w, 1056 w, 1044 w, 1021 w, 935 m, 822 w, 800 m, 770 w, 668 w. Anal. Calcd (%) for $C_{102}H_{140}N_8S_4Sm_2$ (loss of ligated thf and C_6D_6 of solvation, 1907.24): C, 64.23; H, 7.40; N, 5.88. Found: C, 63.21; H, 7.70; N, 5.52.

Synthesis of $[Sm(DippForm)_2(OC(Ph)_2C_2Ph)(thf)]_6$. Toluene (2 mL) was added to a Schlenk flask charged with $[Sm(DippForm)_2(CPh)(thf)]$ (0.54 g, 0.50 mmol) and benzophenone (0.09 g, 0.50 mmol). The mixture was warmed until all reactants were dissolved. The mixture was stored for 1 week, during which time light yellow crystalline 6 precipitated and was collected (yield: 0.40 g, 65%), mp 258–262 °C. IR (Nujol)/ cm^{-1} : 1666 m, 1594 w, 1520 m, 1314 w, 1278 m, 1183 w, 1108 w, 1068 w, 1024 w, 1010 w, 939 w, 868 w, 800 m, 770 w, 754 m, 702 w, 693 w, 656 w, 646 w. ¹H NMR (C_6D_6 , 303 K)/ppm: 14.72 (s, 2H, NC(H)=N), 6.54–9.91 (m, 27H, C_6H_5 + C_6H_5), 3.40 (m, 4H, OCH_2 , thf), 2.09 (s, br, 8H, CH, 'Pr), 1.34 (m, 4H, CH_2 , thf), 0.09 (s, 48H, CH_3 , 'Pr). Anal. Calcd (%) for $C_{75}H_{93}N_4O_2Sm$ (1232.88): C, 73.06; H, 7.60; N, 4.54. Found: C, 73.03; H, 7.56; N, 4.58.

Two large rod-shaped light yellow crystals grew from the solution having different morphology to the rhombic-shaped crystals of 6. They were picked up by hand and identified by X-ray crystal structure determination to be $[Sm(DippForm)_2\{OC(Ph)_2C_2Ph\}]_6 \cdot 0.5PhMe$ (7-0.5PhMe).

X-ray Crystal Structure Determinations. Crystals in viscous paraffin oil were mounted on glass fibers or cryoloops. Intensity data were collected on the Australian Synchrotron MX1 beamline (2-1.25PhMe, 4-1.5PhMe, and 4Yb-2.25thf) at 100 K with wavelength $\lambda = 0.712$ Å or a Bruker X8 APEX II CCD diffractometer (5-6 C_6D_6) or an Enraf-Nonius Kappa CCD diffractometer (6 and 7-0.5PhMe) using Mo $K\alpha$ radiation at 123 K ($\lambda = 0.71073$ Å). With the MX1 beamline, data were collected using the BlueIce^{26a} GUI and processed with the XDS^{26b} software package. Data sets collected from other diffractometers were empirically corrected for absorption with SADABS²⁷ or SORTAV.²⁸ The structures were solved by conventional methods and refined by full-matrix least-squares on all F^2 data using SHELX97²⁹ or SHELX2014 in conjunction with the X-Seed³⁰ or Olex2³¹ graphical

Table 1. Crystal Data and Structure Refinement for Complexes 2 and 4–7

	2·1.2SPhMe	4·2.5PhMe	4Yb·2.25thf
formula	C _{83.75} H ₁₁₅ N ₆ KSm	C _{147.50} H ₁₈₈ N ₈ O ₃ Sm ₂	C ₁₃₉ H ₁₈₆ N ₈ O _{5.25} Yb ₂
<i>M_r</i>	1395.27	2421.76	2399.04
space group	<i>P</i> 2 ₁ / <i>c</i>	<i>P</i> $\bar{1}$	<i>P</i> $\bar{1}$
<i>a</i> (Å)	24.734(5)	24.439(5)	13.792(3)
<i>b</i> (Å)	26.888(5)	25.688(5)	22.820(5)
<i>c</i> (Å)	24.902(5)	25.726(5)	23.442(5)
α (deg)	90	102.65(3)	117.65(3)
β (deg)	111.88(5)	108.63(3)	103.71(3)
γ (deg)	90	112.47(3)	91.51(3)
<i>V</i> (Å ³)	15368(5)	13026(4)	6269(2)
<i>Z</i>	8	4	2
μ , mm ^{−1}	0.864	0.948	1.539
ρ_{calc} g cm ^{−3}	1.206	1.235	1.271
<i>N_r</i>	198965	174813	28645
<i>N</i> (<i>R_{int}</i>)	26829 (0.347)	45749(0.0286)	28645(0.0142)
<i>R</i> 1/ <i>wR</i> 2 (<i>I</i> > 2σ(<i>I</i>))	0.0326/0.0831	0.0620/0.1678	0.0327/0.0788
<i>R</i> 1/ <i>wR</i> 2 (all data)	0.0354/0.0847	0.0667/0.1722	0.0339/0.0794
GOF	1.063	1.056	1.106
max/min Δ <i>e</i> [e·Å ^{−3}]	1.304/−1.076	2.760/−2.174	1.677/−2.081
	5·6C ₆ D ₆	6	7·0.5PhMe
formula	C ₁₄₆ H ₁₉₂ N ₈ O ₂ S ₄ Sm ₂ ^a	C ₇₅ H ₉₃ N ₄ O ₂ Sm	C _{74.5} H ₈₉ N ₄ OSm
<i>M_r</i>	2520.04	1232.88	1206.84
space group	<i>P</i> 2 ₁ / <i>n</i>	<i>P</i> $\bar{1}$	<i>P</i> $\bar{1}$
<i>a</i> (Å)	15.8749(3)	12.937(3)	14.276(3)
<i>b</i> (Å)	23.1663(6)	13.607(3)	14.806(3)
<i>c</i> (Å)	19.3292(3)	20.847(4)	18.060(4)
α (deg)	90	94.09(3)	97.15(3)
β (deg)	107.876(1)	93.12(3)	98.88(3)
γ (deg)	90	116.75(3)	118.30(3)
<i>V</i> (Å ³)	6765.4(2)	3252.1(11)	3233.7(11)
<i>Z</i>	2	2	2
μ , mm ^{−1}	0.974	0.951	0.954
ρ_{calc} g cm ^{−3}	1.255	1.259	1.237
<i>N_r</i>	55165	35717	54056
<i>N</i> (<i>R_{int}</i>)	15525(0.0550)	11037(0.0681)	11382(0.0648)
<i>R</i> 1/ <i>wR</i> 2 (<i>I</i> > 2σ(<i>I</i>))	0.0403/0.0720	0.0444/0.1092	0.0377/0.0956
<i>R</i> 1/ <i>wR</i> 2 (all data)	0.0533/0.0787	0.0536/0.1157	0.0410/0.0989
GOF	1.073	1.074	1.067
max/min Δ <i>e</i> [e·Å ^{−3}]	0.777/−0.850	2.120/−0.959	1.696/−1.015

^aD modeled as H.

user interface. Anisotropic thermal parameters were refined for non-hydrogen atoms, and hydrogen atoms were calculated and refined with a riding model. Crystal data, data collection, and refinement details are given in Table 1.

Crystallographic data (excluding structure factors) for the structures reported in this paper have been deposited with the Cambridge Crystallographic Data Centre as supplementary publication numbers CCDC 1023027–1023033. Copies of the data can be obtained free of charge on application to CCDC, 12 Union Road, Cambridge CB2 1EZ, U.K. (fax, (+44) 1223 336-033; e-mail, deposit@ccdc.cam.ac.uk).

RESULTS AND DISCUSSION

Treatment of the homoleptic formamidinosamarium(III) complex [Sm(DippForm)₃] **1** with potassium graphite at 90 °C yielded a dark brown heterobimetallic formamidinosamarium(II)/potassium complex [KSm(DippForm)₃] **2** in moderate yield (Scheme 2i). C, H, and N elemental analysis for **2** was consistent with the proposed formula, and the molecular structure was confirmed by X-ray crystallography. However, the poor solubility in hydrocarbon

solvents and the paramagnetic nature of the compound prevented an informative NMR spectrum. Previously reported [KLn^{II}L₃] complexes include L = N(SiMe₃)₂, Ln = Yb,^{32a} Sm;^{32b} L = C(SiMe₃)₃, Ln = Yb;^{32c} L = OC₆H₃Ph₂-2,6, Ln = Eu.^{32d}

Complex **2** and the previously reported^{6,25} dark green Sm^{II} complex [Sm(DippForm)₂(thf)₂] **3** are the only known divalent formamidinosamarium species so far reported, and amidinato analogues are rare.¹⁸ **2** is a polymeric heteronuclear samarium(II) species free of Lewis base solvent coordination in contrast to the mononuclear heteroleptic samarium(II) complex **3**. Both formamidinosamarium(II) complexes can be directly (Scheme 2ii) or indirectly (Scheme 2iv+i) transformed into each other, with the key factor being the presence or absence of thf. The addition of thf to **2** leads to breakup of the polymer and the transformation of **2** into **3** (Scheme 2ii). The reduction of the related [Sm(DippForm)₂Cl(thf)]²³ complex by potassium graphite yielded the Lewis base coordinated samarium(II) complex **3**, thf being

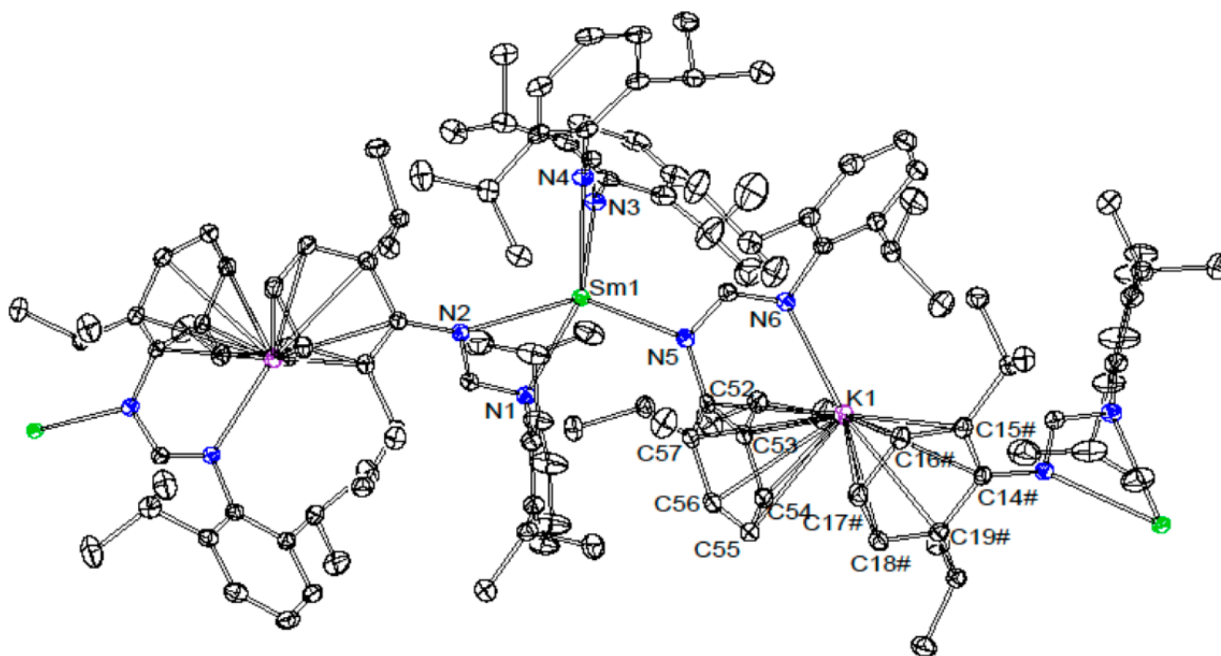
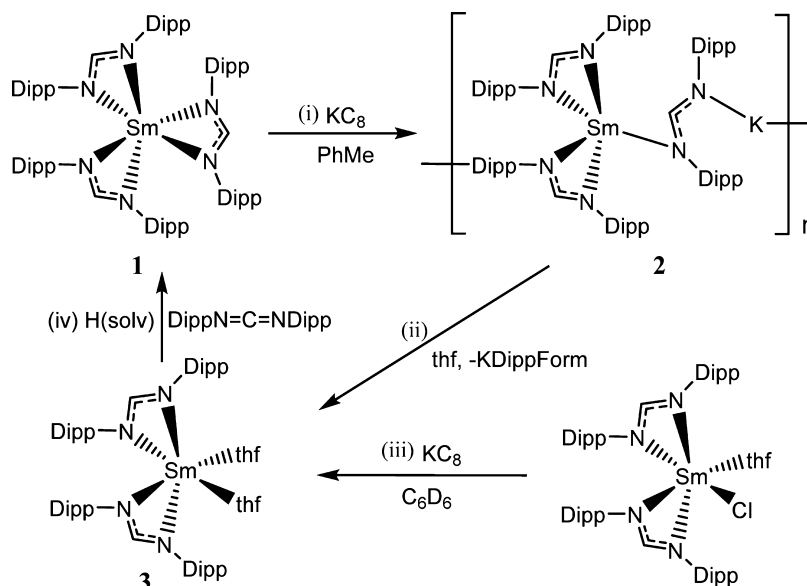
Scheme 2. Synthesis of $[\text{KSm}(\text{DippForm})_3]_n$ **2** and the Transformation of **2** or $[\text{Sm}(\text{DippForm})_2\text{Cl}(\text{thf})]$ into **3**

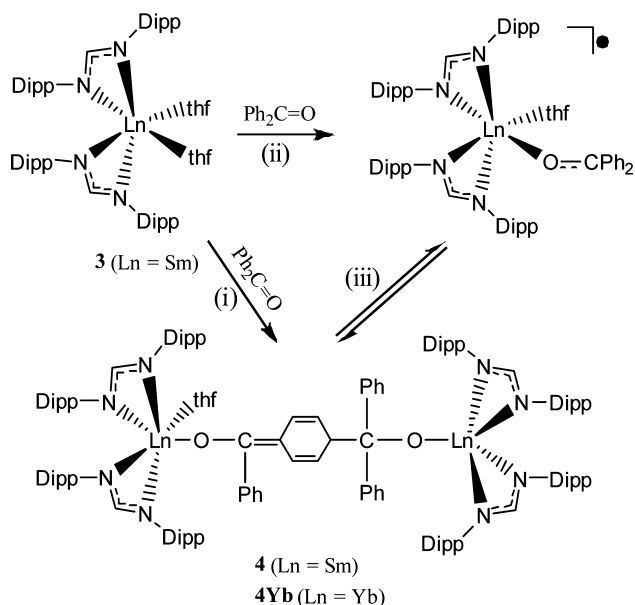
Figure 1. Molecular structure of **2**·1.25PhMe shown with 50% thermal ellipsoids. Lattice toluene molecules and hydrogen atoms omitted for clarity. Selected bond distances (Å) and angles (deg): Sm1–N1 = 2.575(2); Sm1–N2 = 2.641(2); Sm1–N3 = 2.587(2); Sm1–N4 = 2.559(2); Sm1–N5 = 2.557(2); K1–N6 = 2.677(2); K1–C14[#] = 3.294(3); K1–C15[#] = 3.307(3); K1–C16[#] = 3.242(3); K1–C17[#] = 3.182(3); K1–C18[#] = 3.151(3); K1–C19[#] = 3.204(3); K1–C52 = 3.147(3); K1–C53 = 3.231(3); K1–C54 = 3.276(3); K1–C55 = 3.255(3); K1–C56 = 3.184(3); K1–C57 = 3.130(3); K1–centroid η^6 (C52–C57) = 2.88; K1–centroid η^6 (C14[#]–C19[#]) = 2.91; centroid η^6 (C52–C57)–K1–N6 = 81.1°; centroid η^6 (C14[#]–C19[#])–K1–N6 = 145.6°; centroid η^6 (C52–C57)–K1–centroid η^6 (C14[#]–C19[#]) = 123.5. [Symmetry code for C14[#]–C19[#]: $x, 5/2 - y, z - 1/2$].

sourced from the reactant (Scheme 2iii). Complex **1** was originally made by the oxidation of the formamidinosamarium(II) complex **3** by *N,N'*-bis(2,6-diisopropylphenyl)carbodiimide (Scheme 2iv).⁶ Ligation by the three bulky formamidinates prevents additional Lewis base solvent coordination in **1**, from which the Lewis base solvent free complex **2** can be prepared (Scheme 2i).

2 crystallized from toluene in the $P2_1/c$ space group (Table 1). The crystal structure of **2** contains two similar but crystallographically independent molecules, and only one is chosen as representative to describe the structure (Figure 1).

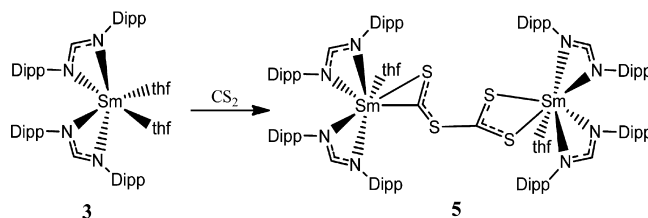
The homoleptic and heteronuclear (Sm/K) complex adopts a one-dimensional polymeric form with alternating Sm and K atoms. Two formamidinate ligands each chelate a samarium atom in a $\kappa(N,N')$ manner, and one also binds to potassium by an η^6 -2,6-diisopropylphenyl group. A third formamidinate bridges Sm and K in a μ - $1\kappa(N):2\kappa(N')$ manner, and the 2,6-diisopropylphenyl group on the nitrogen bound to Sm is η^6 -coordinated to potassium. The samarium atom is thus a low five coordinate, and the coordination geometry can be described as a distorted square pyramid with the unidentate formamidinate nitrogen atom in an apical position. The Sm–N

Scheme 3. Synthesis of $[(\text{DippForm})_2(\text{thf})\text{Ln}\{\mu\text{-OC(Ph)=C(C}_6\text{H}_5\text{)C(Ph)}_2\text{O}\}\text{Ln}(\text{DippForm})_2]$ **4** (Ln = Sm) and **4Yb** (Ln = Yb)



bond length (2.577(2) Å) of the unidentate formamidinate is close to the mean Sm–N value of the chelating formamidinates (2.59 Å) (Figure 1). These bond lengths are comparable to those in the six coordinate samarium(II) complex $[\text{Sm}(\text{DippForm})_2(\text{thf})_2]$ **3** (mean, 2.57 Å)²⁵ despite the difference in coordination number between **2** and **3**. Evidently, formamidinate bridging between two metals (Sm/K) offsets

Scheme 4. Synthesis of $[\{\text{Sm}(\text{DippForm})_2(\text{thf})\}_2(\mu\text{-}\eta^2(\text{C},\text{S});\kappa(\text{S}',\text{S}'')\text{-SCSCS}_2)]$ **5**



the effect of the lower coordination number. The Sm–N bond lengths, as expected,³³ are longer than those of trivalent samarium complexes (e.g., $[\text{Sm}(\text{DippForm})_2\text{Cl}(\text{thf})]$, mean 2.44 Å).²³ The difference between the C–N or C=N bond lengths of the diaza-allyl moiety of each formamidinate ligand increases from $\kappa(\text{N},\text{N}')$ bonding (typically ≤ 0.01 Å) to bridging $1\kappa(\text{N}):2\kappa(\text{N}')$ (ca. 0.03 Å). Samarium and potassium metal atoms are bridged by formamidinate ligands through $1\kappa(\text{N}):2\kappa(\text{N}')$ ligation and η^6 -bonding of aryl substituents. The latter architects a metallocene arrangement around the potassium atom (centroid $\eta^6(\text{C}52\text{--C}57)\text{--K1--centroid}\eta^6(\text{C}14^\#\text{--C}19^\#)$ = 123.5°). The interactions between the seven coordinate potassium atom and arene rings (K1–centroid $\eta^6(\text{C}52\text{--C}57)$ = 2.88 Å and K1–centroid $\eta^6(\text{C}14^\#\text{--C}19^\#)$ = 2.91 Å) are shorter than those of $\eta^6\text{-PhMe}$ of seven coordinate potassium in $[\text{Lu}\{\text{CH}(\text{SiMe}_3)_2\}_3(\mu\text{-Cl})\text{K}(\text{PhMe})_2]$ (3.00–3.13 Å).³⁴ The K–C bond lengths (3.130(3)–3.307(3) Å) are within the range of the $\eta^6\text{-Ar--K}$ interactions in the seven coordinate potassium/samarium complex $[\{\text{Ph}_2\text{Si}(\text{NAr})_2\}_2\text{Sm}^{\text{II}}\{\text{K}(\text{OEt}_2)_2\}_2]$ (3.032(3)–3.456(3) Å).³⁵ The K–N bond caps the sandwich unit asymmetrically with centroid $\eta^6(\text{C}52\text{--C}57)\text{--}$

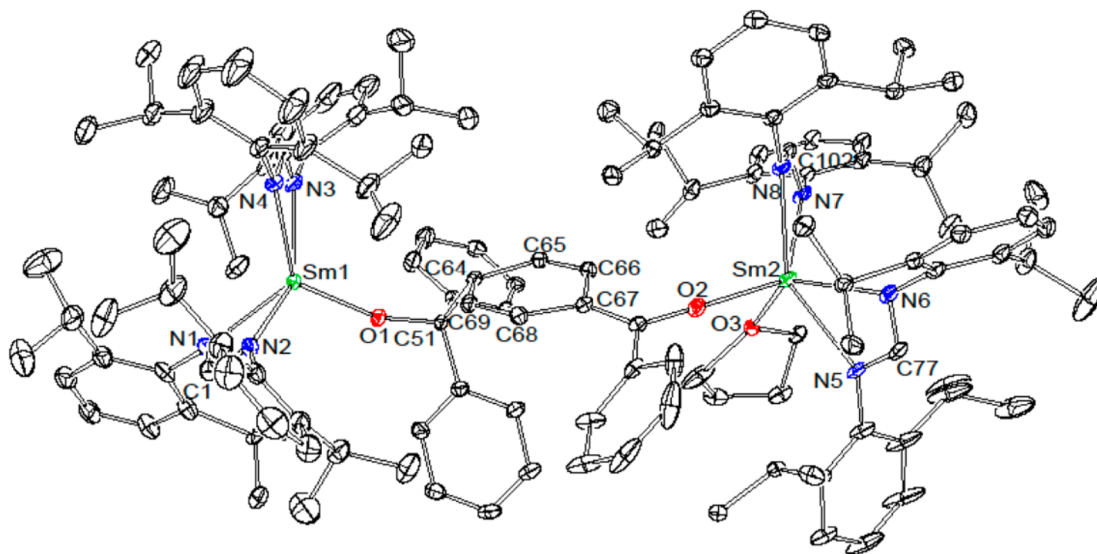


Figure 2. Molecular structure of **4-2.5PhMe** shown with 30% thermal ellipsoids. Hydrogen atoms, lattice solvent, and half of the disordered site omitted for clarity. Selected bond distances (Å) and angles (deg): Sm1–O1 = 2.075(3); Sm1–N1 = 2.381(4); Sm1–N2 = 2.409(4); Sm1–N3 = 2.424(4); Sm1–N4 = 2.434(4); Sm2–O2 = 2.142(3); Sm2–N5 = 2.431(3); Sm2–N6 = 2.501(4); Sm2–N7 = 2.447(4); Sm2–N8 = 2.435(4); C64–C65 = 1.505(6); C64–C69 = 1.506(6); C65–C66 = 1.342(6); C68–C69 = 1.344(6); C66–C67 = 1.455(6); C67–C68 = 1.461(6); C67–C70 = 1.379(6); C1...Sm1...C26 = 128.56(14); C1...Sm1–O1 = 113.83(13); C26...Sm1–O1 = 116.81(13); O2–Sm2–O3 = 86.77(16); C77...Sm2...C102 = 123.94(13). [Relevant bond distances (Å) and angles (deg) for **4Yb-2.25thf**: Yb1–O1 = 2.010(2); Yb1–N1 = 2.317(2); Yb1–N2 = 2.285(2); Yb1–N3 = 2.318(2); Yb1–N4 = 2.351(2); Yb2–O2 = 2.0722(19); Yb2–N5 = 2.391(2); Yb2–N6 = 2.347(3); Yb2–N7 = 2.372(2); Yb2–N8 = 2.356(2); C64–C65 = 1.505(4); C64–C69 = 1.498(4); C65–C66 = 1.335(4); C68–C69 = 1.336(4); C66–C67 = 1.457(4); C67–C68 = 1.458(4); C67–C70 = 1.370(4); C1...Yb1...C26 = 125.92(8); C1...Yb1–O1 = 115.79(9); C26...Yb1–O1 = 118.26(9); O2–Yb2–O3 = 82.97(7); C77...Yb2...C102 = 121.56(8).]

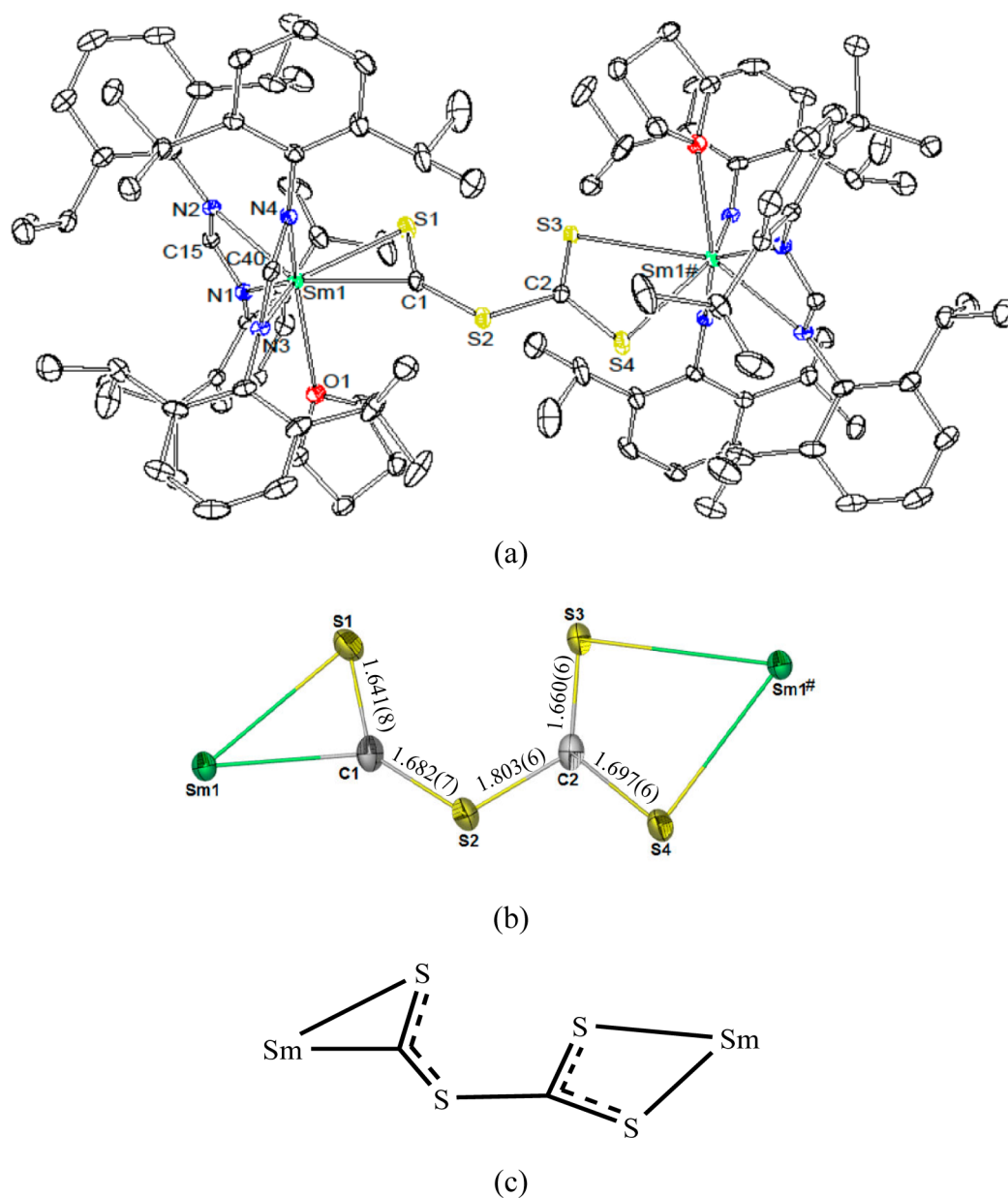
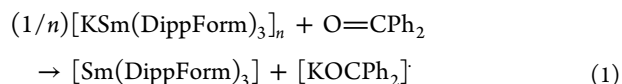


Figure 3. (a) Molecular structure of 5·6C₆D₆ shown with 50% thermal ellipsoids. Hydrogen atoms, lattice solvent, and half of the disordered site omitted for clarity. Selected bond distances (Å) and angles (deg): Sm1–N1 = 2.457(2); Sm1–N2 = 2.482(2); Sm1–N3 = 2.424(2); Sm1–N4 = 2.479(2); Sm1–O1 = 2.4604(18); Sm1–C1 = 2.476(7); Sm1–S1 = 2.7724(18); Sm1#–S3 = 3.0051(18); Sm1#–S4 = 2.9484(19); C1–S1 = 1.641(8); C1–S2 = 1.682(7); C2–S2 = 1.803(6); C2–S3 = 1.659(6); C2–S4 = 1.697(6); S3–Sm1#–S4 = 60.05(6). [Symmetry code for Sm1#: 2 – x, –y, 2 – z.] (b) Central part of the molecular structure of 5·6C₆D₆: Sm1(μ-η²(C,S):κ(S',S''))-SCSCS₂Sm1# core. (c) Central part of the molecular structure in ChemDraw.

K1–N6 = 81.1° and centroid(η^6 (C14#–C19#))–K1–N6 = 145.6°.

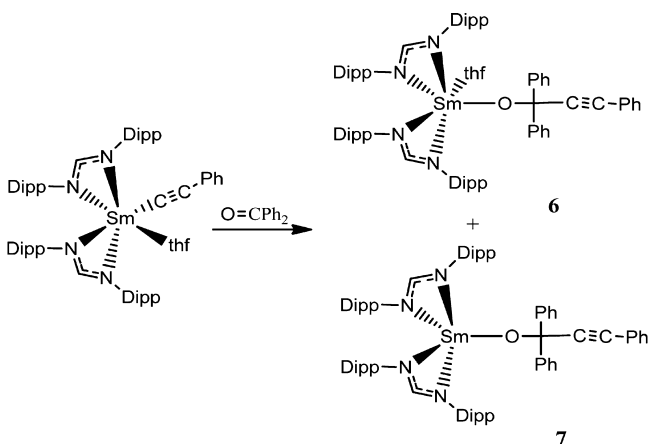
The different constitution of the samarium(II) complexes **2** and **3** is expected to diversify their reactivity. This is observed in their behavior with benzophenone. **2** reacts with benzophenone giving **1** with the plausible coproduct [KOCPh₂][•] (eq 1), which can abstract a hydrogen atom to give KOCHPh₂ or dimerize to the pinacolate [K₂(OCPh₂)₂]. However, the reduction of benzophenone by **3** led to the isolation of the novel heteroleptic dinuclear samarium(III) complex **4** (Scheme 3i). **4** has a pale color in the solid state, but exhibits a purple color when dissolved in toluene. Supposedly, an equilibrium occurs in solution forming a ketyl species (Scheme 3iii), the phenomenon having been observed previously in a related

reaction.⁷ The equilibrium process in solution, along with the paramagnetic effect of the samarium(III) atom, prevents an informative NMR spectrum. However, the formulation of the solid compound was supported by microanalysis, and the structure was clarified by single crystal X-ray structure determination (see below).



The formation of **4** highlights an unusual C–C coupling of the para position of an arene ring with a carbonyl carbon. To examine whether or not this phenomenon is unique to samarium metal, we extended the study to the analogous

Scheme 5. Synthesis of
 $[\text{Sm}(\text{DippForm})_2\{\text{OC}(\text{Ph})_2\text{C}_2\text{Ph}\}(\text{thf})]$ **6** and
 $[\text{Sm}(\text{DippForm})_2\{\text{OC}(\text{Ph})_2\text{C}_2\text{Ph}\}]$ **7**



complex $[\text{Yb}(\text{DippForm})_2(\text{thf})_2]$. Interestingly, the reaction with benzophenone gave a similar product **4Yb**. An equilibrium in solution also occurs forming a purple ketyl species for **4Yb** (Scheme 3iii). The identification of **4Yb** was made by X-ray crystallography, and its structure is very similar to that of **4** (below). A satisfactory elemental microanalysis of **4Yb** was also obtained.

Both compounds **4** and **4Yb** crystallized in the $P\bar{1}$ space groups, and they have similar structures though they are not isomorphous (Table 1 and Figure 2). They adopt dinuclear forms with formamidinate ligands chelating samarium atoms in a $\kappa(N,N')$ manner. The two samarium atoms are joined through two benzophenone molecules coupled from the para position of a benzene ring of one molecule to a carbonyl carbon of the other. The two metal atoms have different coordination numbers: one is five coordinate (Sm1), and the other is six coordinate (Sm2). Consequently, the mean Sm1-N bond length for Sm1 (2.41 Å) is slightly shorter than that of Sm2 (2.45 Å). These Sm-N bonds are longer than Yb-N bonds (mean Yb1-N , 2.32 Å; Yb2-N , 2.37 Å), corresponding to the ionic radius difference between the two metals.³³ If the amidinate ligand is viewed from the position of the backbone carbon (NCN), the coordination geometry of Sm1 or Yb1 can be described as trigonal planar and of Sm2 or Yb2 as distorted tetrahedral. The structure of the new organic moiety in the two complexes is the same (Figure 2). The C–C coupling of the two benzophenone units between one carbonyl carbon and one para position of one arene ring involves formation of a single bond (e.g., $\text{C51-C64} = 1.601(6)$ Å in **4**). There is a loss of aromaticity of arene ring C64-C69 with two adjacent single bonds (C64-C65 , 1.505(6); C64-C69 , 1.506(6) Å in **4**), two further adjacent near single bonds (C66-C67 , 1.454(6); C67-C68 , 1.461(6) Å in **4**) and two cross ring near double bonds (C65-C66 , 1.342(6); C68-C69 , 1.344(6) Å in **4**). There is a partial double bond from the ring C67 to exocyclic C70 (1.379(6) Å). The nonaromatic nature of six membered ring $\text{C}(64-69)$ is further shown by the location of a substituent C51 displaced from the ring plane by 1.284 Å (in **4**). Compound **4Yb** shows similar structural features. This type of C–C coupling is extremely rare and has been observed only once in f-block chemistry benzophenone was reduced by a U^{III} complex,^{36a} where the coupled species was only a minor product, unlike the major products, **4**, **4Yb**. There is also a very

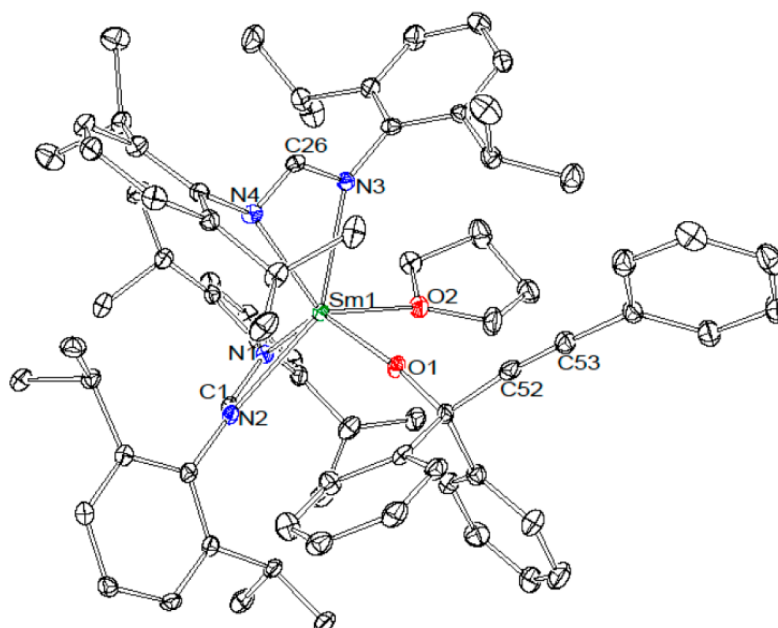
recent example in d-block chemistry involving a Co–Zr bimetallic.^{36b} These reactions differ from most other reductive C–C coupling reactions of benzophenone, which usually occur at two carbonyl carbon atoms forming pinacolate ligands.^{11,12}

The current unusual coupling behavior is an extension of previously observed C–C coupling of $\text{ArN}=\text{C}=\text{NAr}$ ($\text{Ar} = 2,6$ -diisopropylphenyl) fragments at two methine carbon atoms of the ^iPr group (Scheme 1ii).⁵ Both processes probably result from the very bulky nature of the N,N' -bis(2,6-diisopropylphenyl)formamidinate ligand (or N,N' -bis(2,6-diisopropylphenyl)carbodiimide). A different loss of aromaticity of benzophenone caused by lanthanoid metals is observed in formation of enolate complexes,³⁷ and dearomatization of pyridine was observed recently in a reaction of $[\text{Sm}(\text{Cp}^*_2)(\text{thf})_2]$ with pyridine forming $[\{\text{Cp}^*_2\text{Sm}(\text{C}_5\text{H}_5\text{N})\}_2\{\mu-(\text{NC}_5\text{H}_5-\text{C}_5\text{H}_5\text{N})\}]]$.³⁸

The redox reaction of **3** with carbon disulfide yielded a samarium(III) complex **5** with a rare thioformyl carbonotriothioate ($(\text{SCSCS}_2)^{2-}$) bridging ligand (rather than a tetrathiooxalate ligand) in moderate yield (Scheme 4). The poor solubility of the compound in hydrocarbon solvent prevented NMR characterization. However, its constitution was supported by microanalysis (after loss of coordinated *thf* and C_6D_6 of solvation under vacuum). The molecular structure has been determined by single crystal X-ray crystallography.

Dinuclear compound **5** crystallized from C_6D_6 in the $P2_1/n$ space group (Table 1), and the molecular structure is shown in Figure 3a. The formamidinate ligands chelate (N,N') seven coordinate samarium atoms with a mean Sm-N bond length of 2.46 Å, which is close to the average Sm-N (2.45 Å) of the six coordinate samarium atom in the dinuclear samarium(III) complex **4**, the combined steric/electronic effect of the less bulky chelating $(\text{SCSCS}_2)^{2-}$ in **5** contrasting that of the bulky unidentate dialkoxide ligand in **4**. If the amidinate ligand is treated as a single donor located on the backbone carbon (NCN), the coordination geometry of the samarium atoms can be described as capped distorted tetrahedral (C15C40O1C1Sm1 or $\text{C15}^\# \text{C40}^\# \text{O1}^\# \text{S4Sm1}^\#$) with Sm-S1 or Sm-S3 bonds capping one face of each tetrahedron. The asymmetric $(\text{SCSCS}_2)^{2-}$ ligand is disordered evenly over two sites (SCSCS_2) and (S_2CSCS). As a result, the molecule has crystallographic symmetry with an inversion center in the midpoint of the two samarium array. The bonding modes related to the central disamarium thioformylcarbonotriothioate fragment $\text{Sm1}(\text{SCSCS}_2)\text{Sm1}^\#$ are shown in Figure 3b and Figure 3c. One $\text{C}=\text{S}$ group has an η^2 -interaction with one samarium atom while the CS_2 fragment chelates the other samarium atom through two sulfur donors. Two CS_2 moieties are coupled through a single bond ($\text{C2-S2} = 1.803(6)$ Å), and the bond length is comparable with that (1.778(12) Å) of $[(\text{Giso})_2\text{Sm}(\mu-\eta^2(\text{C,S}):\kappa(\text{S}',\text{S}'')-\text{SCSCS}_2)\text{Sm}(\text{Giso})_2]$.^{15a} Electrons of the $\text{S}=\text{C}$ bonds are delocalized over the CS_2 or SCS units since their C–S bond lengths (1.640(7)–1.698(6) Å) are in a range between single and double bonds, though C1-S1 approaches a double bond value (~ 1.60 Å). These values are somewhat shorter than those of related $[\text{Cp}^*_2\text{Sm}(\kappa(\text{S,S}')-\text{S}_2\text{CCH}=\text{CHCH}_3)]$ (S-C bond lengths, 1.693(13) and 1.703(12) Å).³⁹ As obtained from XRD data of good quality (Table 1), the current bond length values of the structure of **5** are more precise (with lower esd values) and assist more in determining the bonding mode of the central carbon–sulfide fragment than those of the recently reported $[(\text{Giso})_2\text{Sm}(\mu-\eta^2(\text{C,S}):\kappa(\text{S}',\text{S}'')-\text{SCSCS}_2)\text{Sm}(\text{Giso})_2]$.^{15a} In the

(a):



(b):

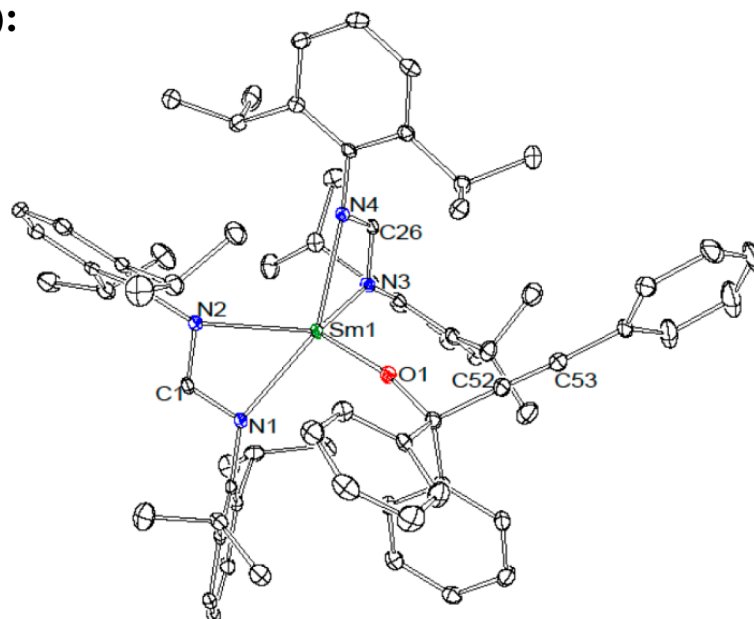


Figure 4. (a) Molecular structure of **6** shown with 50% thermal ellipsoids. Hydrogen atoms omitted for clarity. Selected bond distances (Å) and angles (deg): Sm1–O1 = 2.100(2); Sm1–O2 = 2.473(3); Sm1–N1 = 2.459(3); Sm1–N2 = 2.553(3); Sm1–N3 = 2.491(3); Sm1–N4 = 2.497(3); C1...Sm1...C26 = 128.18(10); C1...Sm1–O1 = 114.04(12); C26...Sm1–O1 = 113.09(11); O1–Sm1–O2 = 84.65(10). (b) Molecular structure of **7·0.5PhMe** shown with 50% thermal ellipsoids. Lattice toluene molecules and hydrogen atoms omitted for clarity. Selected bond distances (Å) and angles (deg): Sm1–O1 = 2.089(2); Sm1–N1 = 2.434(3); Sm1–N2 = 2.464(2); Sm1–N3 = 2.392(2); Sm1–N4 = 2.440(2); C1...Sm1...C26 = 132.08(8); C1...Sm1–O1 = 109.80(9); C26...Sm1–O1 = 118.10(8).

present structure, electron delocalization in the S1C1S2 and S3C2S4 units is clear and S2–C2 is a single bond. However, the overall pattern of bond lengths in both structures is the same, and in particular the Sm–S distance in the Sm–C(S) chelate is shorter than those of the Sm–S₂ chelate (Figure 3). The reaction of **3** with CS₂ (Scheme 4) contrasts with a recent report of the corresponding reaction of [K₂Ln^{II}(OSi(OⁱBu)₃)₄] (Ln = Eu, Yb, see Introduction). Preliminary results indicate that [Yb(DippForm)₂(thf)₂] reacts differently from **3**, and this is an ongoing investigation.⁴⁰

In contrast to the redox reactions between samarium(II) complexes such as **2** and **3** with benzophenone, phenylethynylbis(*N,N'*-bis(2,6-diisopropylphenyl)-formamidinato)tetrahydrofuransamarium(III) activates the C=O bond by insertion (Scheme 5). Thus, it reacts with benzophenone in toluene at ambient temperature, yielding the light yellow alkoxide [Sm(DippForm)₂(OC(Ph)₂C₂Ph)(thf)] **6** in good yield. A minor unsolvated product, [Sm(DippForm)₂(OC(Ph)₂C₂Ph)] **7**, was isolated by hand picking from the bulk crystalline material. Compound **6** is very soluble

in hydrocarbon solvents such as toluene and benzene. The constitution of the compound was supported by NMR characterization and C, H, and N elemental analysis. The molecular structures of both **6** and the unsolvated coproduct **7** were determined by single crystal crystallography (see below). The low yield of **7** prevented any further characterization.

Both bis(formamidinato)samarium complexes crystallized from toluene in the $P\bar{1}$ space group (Table 1), and their molecular structures are shown in Figure 4a (**6**) and Figure 4b (**7**). In these monomeric and heteroleptic species, the stereochemistry of the coordination of samarium metals can be described as distorted tetrahedral (for six coordinate **6**) and trigonal planar (for five coordinate **7**) if the amidinate ligand is treated as a single donor ligand on the NCN carbon. The formamidinate ligands are $\kappa(N,N')$ bonded to the samarium metal as in **4** and **5**, with the average Sm–N bond length (2.50 Å) in **6** somewhat longer than for the six coordinate Sm2 atom in **4** (2.45 Å) and in $[\text{Sm}(\text{DippForm})_2\text{Cl}(\text{thf})]$ (2.44 Å),²³ owing to the bulky alkoxy ligand. The molecular structure of complex **7** is similar to that of the major product **6**, except for an absence of Lewis base thf coordination. As a consequence, the mean Sm–N bond length (2.43 Å) and Sm–O (alkoxy) (2.089(2) Å) bond in **7** are shorter or slightly shorter than those of **6** (Sm–N, 2.50 Å and Sm–O (alkoxy), 2.100(2) Å). The variation in the structures reflects the combined bulk of the alkoxy group ($\text{OCPh}_2(\text{CCPh})$) and the two formamidinate ligands, which leads to labile Lewis base coordination. Related insertion reactions of alkylsamarium complexes with benzophenone are known, and the bulkiness of resulting alkoxide ligand can exclude the coordination of Lewis base solvent, e.g., $[\text{Cp}^*_2\text{SmOCPh}_2(\text{SiH}_3)]$.⁴¹

CONCLUSION

The formation of a novel heteronuclear and homoleptic samarium(II) complex $[\text{KS}(\text{DippForm})_3]_n$ **2** shows that the bulky formamidinates are able to stabilize both samarium and potassium metals in a heteronuclear species without the need for coligands. The varied constitution of divalent samarium(II) complexes **2** and **3** diversifies their redox reactivity, as demonstrated by the reactions with benzophenone. The redox reactivity of $[\text{Sm}(\text{DippForm})_2(\text{thf})_2]$ **3** with C=O/C=S bonds instigates C–C or C–S coupling. The unusual C–C coupling forming **4** is not unique to samarium metal since a parallel reaction occurs for ytterbium forming **4Yb**. Both **4** and **4Yb** feature an isomer of the phenyl group in the bridging ligand. Reaction of **3** with CS_2 leads to the unusual $[\text{SCSCS}_2]^-$ bridging ligand. The organometallic samarium(III) complex, $[\text{Sm}(\text{DippForm})_2(\text{CCPh})(\text{thf})]$, activates the C=O bonds of Ph_2CO in an insertion reaction giving new heteroleptic alkoxoformamidinosamarium(III) complexes, **6** and **7**, which contrast the unusual oxidation products, **4**, **4Yb**, and **5**.

ASSOCIATED CONTENT

Supporting Information

Selected X-ray crystal data information in CIF format. This material is available free of charge via the Internet at <http://pubs.acs.org>.

AUTHOR INFORMATION

Corresponding Authors

*(G.B.D.) E-mail: glen.deacon@monash.edu. Fax: (+61) 399054597.

*(P.C.J.) E-mail: peter.junk@jcu.edu.au. Fax: (+61) 747816078.

Notes

The authors declare no competing financial interest.

ACKNOWLEDGMENTS

This work was supported by the Australian Research Council (Grant DP130100152) and Australian Postgraduate Award (to D.W.). Some aspects of this research were undertaken on the MX1 beamline at the Australian Synchrotron, Victoria, Australia.

DEDICATION

[#]This paper is dedicated to the memory of Professor John Corbett, a solid state chemist of the highest caliber.

REFERENCES

- (1) (a) Bochkarev, M. N.; Zakharov, L. N.; Kalinina, G. S. *Organoderivatives of Rare Earth Elements*; Kluwer Academic: Dordrecht, The Netherlands, 1995. (b) Kobayashi, S., Ed. *Lanthanides: Chemistry and Use in Organic Synthesis*. In *Topics in Organometallic Chemistry*; Springer: Berlin, 1999; Vol. 2. (c) Huang, C.-H., Ed. *Rare Earth Coordination Chemistry: Fundamentals and Applications*; Wiley: Oxford, U.K., 2010.
- (2) (a) Girard, P.; Namy, J. L.; Kagan, H. B. *J. Am. Chem. Soc.* **1980**, *102*, 2693–2698. (b) Molander, G. A. *Org. React.* **2004**, *46*, 211–367. (c) Procter, D. J.; Flowers, R. A.; Skrydstrup, T. *Organic Synthesis Using Samarium Diiodide: A Practical Guide*; Royal Society of Chemistry Publishing, U.K., 2010.
- (3) (a) Morss, L. R. *Chem. Rev.* **1976**, *76*, 827–841. (b) Bond, A. M.; Deacon, G. B.; Newnham, R. H. *Organometallics* **1986**, *5*, 2312–2316.
- (4) (a) Evans, W. J.; Ulibarri, T. A.; Ziller, J. W. *J. Am. Chem. Soc.* **1988**, *110*, 6877–6883. (b) Berube, C. D.; Yazdanbakhsh, M.; Gambarotta, S.; Yap, G. P. A. *Organometallics* **2003**, *22*, 3742–3747. (c) Dube, T.; Ganesan, M.; Conoci, S.; Gambarotta, S.; Yap, G. P. A. *Organometallics* **2000**, *19*, 3716–3721. (d) Dube, T.; Conoci, S.; Gambarotta, S.; Yap, G. P. A.; Vasapollo, G. *Angew. Chem., Int. Ed.* **1999**, *38*, 3657–3659. (e) Jubbs, J.; Gambarotta, S. *J. Am. Chem. Soc.* **1994**, *116*, 4477–4478. (f) Guan, J.-W.; Dube, T.; Gambarotta, S.; Yap, G. P. A. *Organometallics* **2000**, *19*, 4820–4827. (g) Guillemot, G.; Castellano, B.; Prange, T.; Solari, E.; Floriani, C. *Inorg. Chem.* **2007**, *46*, 5152–5154. (h) Gardiner, M. G.; Stringer, D. N. *Materials* **2010**, *3*, 841–862. (i) $\text{N}\equiv\text{N}$ bond can be also reduced by other divalent rare earth metals, for examples, see: Fieser, M. E.; Bates, J. E.; Ziller, J. W.; Furche, F.; Evans, W. J. *J. Am. Chem. Soc.* **2013**, *135*, 3804–3807. (j) Evans, W. J.; Allen, N. T.; Ziller, J. W. *Angew. Chem., Int. Ed.* **2002**, *41*, 359–361. (k) Jaroschik, F.; Momin, A.; Nief, F.; Le Goff, X.-F.; Deacon, G. B.; Junk, P. C. *Angew. Chem., Int. Ed.* **2009**, *48*, 1117–1121.
- (5) Deacon, G. B.; Forsyth, C. M.; Junk, P. C.; Wang, J. *Inorg. Chem.* **2007**, *46*, 10022–10030.
- (6) Cole, M. L.; Deacon, G. B.; Forsyth, C. M.; Junk, P. C.; Polo, D. C.; Wang, J. *Dalton Trans.* **2010**, *39*, 6732–6738.
- (7) Hou, Z.; Fujita, A.; Yamazaki, H.; Wakatsuki, Y. *J. Am. Chem. Soc.* **1996**, *118*, 7843–7844.
- (8) Hou, Z.; Fujita, A.; Zhang, Y.; Miyano, T.; Yamazaki, H.; Wakatsuki, Y. *J. Am. Chem. Soc.* **1998**, *120*, 754–766.
- (9) Clegg, W.; Eaborn, C.; Izod, K.; O'Shaughnessy, P.; Smith, J. D. *Angew. Chem., Int. Ed. Engl.* **1997**, *36*, 2815–2817.
- (10) Tardif, O.; Hou, Z.-M.; Nishiura, M.; Koizumi, T.-A.; Wakatsuki, Y. *Organometallics* **2001**, *20*, 4565–4573.
- (11) Deacon, G. B.; Forsyth, C. M.; Wilkinson, D. L. *Chem.—Eur. J.* **2001**, *7*, 1784–1795.
- (12) Fedushkin, I. L.; Skatova, A. A.; Cherkasov, V. K.; Chudakova, V. A.; Dechert, S.; Hummert, M.; Schumann, H. *Chem.—Eur. J.* **2003**, *9*, 5778–5783.
- (13) (a) Evans, W. J.; Seibel, C. A.; Ziller, J. W. *Inorg. Chem.* **1998**, *37*, 770–776. (b) Castro, L.; Labouille, S.; Kindra, D. R.; Ziller, J. W.; Nief, F.; Evans, W. J.; Maron, L. *Chem.—Eur. J.* **2012**, *18*, 7886–7895.

- (14) Davies, N. W.; Frey, A. S. P.; Gardiner, M. G.; Wang, J. *Chem. Commun.* **2006**, 4853–4855.
- (15) (a) Heitmann, D.; Jones, C.; Mills, D. P.; Stasch, A. *Dalton Trans.* **2010**, 39, 1877–1882. Note: The authors state in their manuscript “...the metrical parameters of the fragment should not be considered as fully reliable. Therefore, it is difficult to confidently discuss the degree of double bond delocalisation over the fragment...” (b) Andrez, J.; Pécaut, J.; Bayle, P.-A.; Mazzanti, M. *Angew. Chem., Int. Ed.* **2014**, 53, 10448–10452.
- (16) See, for example: (a) Cromhout, N. L.; Manning, A. R.; McAdam, C. J.; Palmer, A. J.; Rieger, A. L.; Reiger, P. H.; Robinson, B. H.; Simpson, J. *Dalton Trans.* **2003**, 2224–2230. (b) Christou, V.; Wuller, S. P.; Arnold, J. J. *Am. Chem. Soc.* **1993**, 115, 10545–10552.
- (17) See, for example: (a) Cowie, M.; Dwight, S. K. *J. Organomet. Chem.* **1981**, 214, 233–252. (b) Werner, H.; Kolb, O.; Feser, R.; Schubert, U. *J. Organomet. Chem.* **1980**, 191, 283–293.
- (18) See reviews, for example: (a) Edelmann, F. T. *Adv. Organomet. Chem.* **2013**, 61, 55–374. (b) Edelmann, F. T. *Chem. Soc. Rev.* **2012**, 41, 7657–7672. (c) Edelmann, F. T. *Chem. Soc. Rev.* **2009**, 38, 2253–2268. (d) Edelmann, F. T. *Adv. Organomet. Chem.* **2008**, 57, 183–352.
- (19) Bergbreiter, D. E.; Killough, J. M. *J. Am. Chem. Soc.* **1978**, 29, 2126–2134.
- (20) Roberts, R. M. *J. Am. Chem. Soc.* **1949**, 71, 3848–3849.
- (21) Namy, J. L.; Girard, P.; Kagan, H. B.; Caro, P. E. *Nouv. J. Chim.* **1981**, 5, 479–484.
- (22) Cole, M. L.; Deacon, G. B.; Forsyth, C. M.; Junk, P. C.; Konstas, K.; Wang, J.; Bittig, H.; Werner, D. *Chem.—Eur. J.* **2013**, 19, 1410–1420.
- (23) Cole, M. L.; Deacon, G. B.; Junk, P. C.; Wang, J. *Organometallics* **2013**, 32, 1370–1378.
- (24) Cole, M. L.; Deacon, G. B.; Forsyth, C. M.; Junk, P. C.; Konstas, K.; Wang, J. *Chem.—Eur. J.* **2007**, 13, 8092–8110.
- (25) Cole, M. L.; Junk, P. C. *Chem. Commun.* **2005**, 2695–2697.
- (26) (a) McPhillips, T. M.; McPhillips, S. E.; Chiu, H. J.; Cohen, A. E.; Deacon, A. M.; Ellis, P. J.; Garman, E.; Gonzalez, A.; Sauter, N. K.; Phizackerley, R. P.; Soltis, S. M.; Kuhn, P. J. *Synchrotron Radiat.* **2002**, 9, 401–406. (b) Kabsch, W. *J. Appl. Crystallogr.* **1993**, 26, 795–800.
- (27) Sheldrick, G. M. *SADABS: Program for scaling and absorption correction of area detector data*; Universität Göttingen: Göttingen, Germany, 1997.
- (28) Blessing, R. H. *J. Appl. Crystallogr.* **1997**, 30, 421–426.
- (29) Sheldrick, G. M. *SHELXL-97, Program for crystal structure refinement*; University of Göttingen: Göttingen, Germany, 1997.
- (30) Barbour, L. J. *J. Supramol. Chem.* **2001**, 1, 189–191.
- (31) Dolomanov, O. V.; Bourhis, L. J.; Gildea, R. J.; Howard, J. A. K.; Puschmann, H. *J. Appl. Crystallogr.* **2009**, 42, 339–341.
- (32) (a) Niemeyer, M. *Inorg. Chem.* **2006**, 45, 9085–9095. (b) Evans, W. J.; Johnstons, M. A.; Clark, R. D.; Anwender, R.; Ziller, J. W. *Polyhedron* **2001**, 20, 2483–2490. (c) Hitchcock, P. B.; Khrostov, A. V.; Lappert, M. F. *J. Organomet. Chem.* **2002**, 663, 263–268. (d) Deacon, G. B.; Junk, P. C.; Moxey, G. J. *Chem.—Asian J.* **2009**, 4, 1309–1317.
- (33) Shannon, R. D. *Acta Crystallogr., Sect. A* **1976**, 32, 751–767.
- (34) Schaverien, C. J.; Mechelen, J. B. V. *Organometallics* **1991**, 10, 1704–1709.
- (35) Pan, C.-L.; Chen, W.; Song, J.-F. *Organometallics* **2011**, 30, 2252–2260.
- (36) (a) Lam, O. P.; Anthon, C.; Heinemann, F. W.; O'Connor, J. M.; Meyer, K. *J. Am. Chem. Soc.* **2008**, 130, 6567–6576. (b) Zhou, W.; Marquard, S. L.; Bezpalko, M. W.; Foxman, B. M.; Thomas, C. M. *Organometallics* **2013**, 32, 1766–1772.
- (37) (a) Hou, Z.; Yoshimura, T.; Wakatsuki, Y. *J. Am. Chem. Soc.* **1994**, 116, 11169–11170. (b) Yoshimura, T.; Hou, Z.; Wakatsuki, Y. *Organometallics* **1995**, 14, 5382–5392.
- (38) Labouille, S.; Nief, F.; Goff, X.-F. L.; Maron, L.; Kindra, D. R.; Houghton, H. L.; Ziller, J. W.; Evans, W. J. *Organometallics* **2012**, 31, 5196–5203.
- (39) Evans, W. J.; Seibel, C. A.; Ziller, J. W.; Doedens, R. J. *Organometallics* **1998**, 17, 2103–2112.
- (40) Deacon, G. B.; Junk, P. C.; Werner, D. **2014**, unpublished results.
- (41) Castillo, I.; Tilley, T. D. *Organometallics* **2000**, 19, 4733–4739.